Assessment of Virtual-Voltage-based Model Predictive Controllers in Six-phase Drives under Open-Phase Faults

I. González-Prieto, M. J. Durán, M. Bermúdez, F. Barrero and C. Martín

***Abstract*— The inherent fault-tolerant capability of multiphase machines is highly appreciated, but it requires fault detection and localization together with a reconfiguration of the control scheme. When the multiphase machine is regulated using finite-control set model predictive control (MPC) strategies, the reconfiguration involves the use of different transformation matrices, cost functions and current references for each of the multiple open-phase fault (OPF) scenarios. Aiming to simplify this procedure and add further robustness, this paper explores the possibility to achieve a natural fault-tolerant capability by maintaining the pre-fault control strategy after the fault occurrence. For this purpose, this work firstly analyzes the two main reasons why MPC-regulated multiphase drives misbehave in the event of an OPF: the voltage vector shifting and the search for incompatible goals. In a next step, a version of the MPC that includes virtual voltage vectors (VVs) is tested for the first time in post-fault situation and it is compared to conventional MPC technique. Extensive experimental results reveal that, while MPC misbehaves in the event of an OPF, the VV-MPC provides a satisfactory ripple-free post-fault performance. This finding has two significant implications for industrial applications: the post-fault operation is highly simplified and, at the same time, the fault-tolerant multiphase drive becomes immune to fault detection errors and delays.**

Keywords*— Model predictive control, post-fault operation, six-phase induction machines, virtual voltage vectors.

I. Introduction

Either operating as a motor or as a generator, any application where the electric machine is supplied from power converters can freely select the most suitable number of stator phases. Both in autonomous (e.g. ship or electric vehicle propulsion) and grid-connected (e.g. wind energy conversion systems) applications, the use of three-phase machines is the standard option, but multiphase machines (more than three phases) can be a better option to satisfy motor/generator specific requirements. High power/currents systems and cases when security becomes critical are good examples of applications where the use of multiphase machines can be advantageous [1-4]. Ship propulsion and wind energy systems can be classified as high-power systems [1,5], whereas aerospace systems require redundancy to ensure the continuous operation [6]. In both cases there are industrial products based on multiphase induction and permanent magnet machines [7].

This work was supported by the Spanish Ministry of Science, Innovation and Universities under Project RTI2018-096151-B-100.

I. Gonzalez-Prieto, M.J. Duran are with the Department of Electrical Engineering at the University of Malaga, Spain, e-mail: ignaciogp87@gmail.com and mjduran@uma.es

M. Bermudez is with the Department of Electrical Engineering at the University of Huelva, Spain, email: mariobermg@gmail.com.

F. Barrero and C. Martin are with the Department of Electronic Engineering at the University of Seville, Spain, e-mail: fbarrero@us.es and cmartin15@us.es.

Among different benefits of the extra phases, the inherent fault-tolerant capability without additional hardware is likely the most appreciated feature, and much work has been done in recent years to investigate the fault-tolerant operation of different types of multiphase machines. From design to control aspects, recent literature has covered different aspects that allow the drive to be self-reconfigurable and provide self-healing properties [1,2]. The reconfiguration typically involves the detection and localization of the fault in a first stage, and the modification of the control scheme in a second stage. Three-phase techniques have been adopted for fault detection purposes [8-9], but another bunch of new techniques that can be exclusively applied together with multiphase systems have also appeared [10-12]. As for the control strategies, the standard techniques in pre-fault situation have also been modified to become fault-tolerant [13-22]. The field-oriented control (FOC) has been reconfigured using different kind of controllers and current references [13-14,19-21], the direct torque control (DTC) has presented new look-up tables that are suitable in post-fault condition [15-16] and model predictive control (MPC) has presented new transformation matrices and cost functions to allow post-fault operation [17-18]. In all cases it is necessary to derate the drive, and some studies have also been devoted to investigate the degree of derating that is obtained under different circumstances [19-21].

In spite of the successful application of these control reconfigurations, they require at least one fault index per phase [12] in order to localize the faulty phase(s). Furthermore, the changes in the control strategy are always dependent on the type of fault. Focusing on open-phase faults (OPFs), which are the most widely studied type of faults in literature [6,13-23], it is still necessary to distinguish between single and multiple faults and consider all fault scenarios. For single faults, this implies one different reconfiguration per phase and in cases with multiple faults it is necessary to take into account all different fault combinations, this providing additional complexity to the fault-tolerant operation. At this stage, it is worth wondering if one can simply maintain the pre-fault control strategy after the fault occurrence with rather satisfactory results. If the answer is yes, the fault-tolerant process would be highly simplified, and it would be possible to achieve a natural fault-tolerant capability without software reconfiguration in the control scheme. This work aims at exploring this possibility and eventually demonstrate if any of the predictive techniques existing in literature can be useful both in pre- and post-fault scenarios.

It is well-known that the standard version of finite-control set model-based predictive control (MPC) misbehaves in the event of an OPF. High current ripples have been reported if the control scheme is not quickly reconfigured after the OPF

occurrence [18]. Nevertheless, the MPC performance has been recently enhanced with the use of virtual voltage vectors (VVs) [24-25]. The virtual/synthetic vectors have been suggested in [26-30] to better regulate the appearance of secondary currents by simply combining two switching states to nullify the x-y voltage production. Even though it has been proved in [24-28] that the use of VVs can improve the current quality, the analysis of all these works has been exclusively confined to the healthy operation of the drive.

This work verifies for the first time the post-fault performance of VV-MPC and provides a comparative analysis with conventional MPC. The comparative results reveal that, contrary to what occurs with MPC, the VV-MPC provides the six-phase drive with a natural fault-tolerant capability that allows a satisfactory ripple-free post-fault performance even with no reconfiguration of the control strategy (just modifying the derating limit). This finding is accompanied with an analysis of the physical phenomena that explains why VV-MPC can satisfactorily operate after the fault occurrence and MPC cannot. Specifically, the main contributions of the investigation are:

C1) The pre-fault MPC strategies are analysed and the two main causes of error after the fault occurrence are identified. The analysis shows how the voltage vectors and virtual voltage vectors are shifted after the OPF occurrence and how the MPC searches for incompatible goals in the regulation of the phase currents.

C2) A comparative analysis is carried out considering different MPC methods without modifying the pre-fault control structure. Extensive experimental results provide a full picture of the performance in pre-fault steady-state, in post-fault steady-state, in the transition from pre- to post-fault situations and in different dynamic conditions.

C3) Based on the previous analysis and experimental tests, it is confirmed that the use of VVs provides a natural fault-tolerant capability without initial software reconfiguration.

While C1 helps to obtain a better insight into the physical phenomena that forces a reconfiguration in some control strategies, C2 extends the analysis of MPC and VV-MPC from healthy condition to situations facing open-phase faults. C3 finally reveals that the VV-MPC can successfully skip the fault localization and control reconfiguration achieving a universal MPC technique that can be used in normal and faulty operation of the multiphase drive.

It must be highlighted that all open-phase post-fault methods for multiphase machines that can be found in literature require either the reconfiguration of the control structure or the recalculation of the current references. On the contrary, the use of VV-MPC techniques proves to provide a natural fault-tolerant capability to the drive because it is possible to operate the system in post-fault mode without changing the control structure and the current references.

The paper is organized as follows. Next section details the six-phase induction motor drive, which represents the multiphase electromechanical system under study. Section III focuses on the conceptual basis of the MPC technique in six-phase induction motor drives. Section IV analyses pre- and post-fault operation of the drive from the theoretical perspective, while experimental results provided in section V confirm the ability of the VV-MPC controller to manage the fault appearance. Conclusions are finally summarized in the last section.

II. Generalities of Six-Phase Induction Motor Drives

A. Topology

With the aim to obtain a certain degree of fault tolerance, a multiphase drive topology that includes a six-phase induction machine (IM) fed by a dual three-phase voltage source converter (VSC) is employed (see Fig. 1). The IM is configured with two isolated neutrals to improve the utilization of the dc-bus voltage and simplify the control stage, this being the most commonly topology in literature [2]. The VSCs are connected to a single dc-link and this provides 2^6= 64 switching states. These switching states can be expressed as a vector $[S]=\{S_{a1},S_{b1},S_{c1},S_{a2},S_{b2},S_{c2}\}$ where the switching state of each VSC leg is defined by S_i. If the upper switch of the leg is ON S_i=1, whereas if the lower switch of the leg is OFF S_i=0. Using this switching state vector, the stator phase voltages can be calculated as follows:

$$\begin{bmatrix} v_{a1} \\ v_{b1} \\ v_{c1} \\ v_{a2} \\ v_{b2} \\ v_{c2} \end{bmatrix} = \frac{V_{dc}}{3} \cdot \begin{bmatrix} 2 & -1 & -1 & 0 & 0 & 0 \\ -1 & 2 & -1 & 0 & 0 & 0 \\ -1 & -1 & 2 & 0 & 0 & 0 \\ 0 & 0 & 0 & 2 & -1 & -1 \\ 0 & 0 & 0 & -1 & 2 & -1 \\ 0 & 0 & 0 & -1 & -1 & 2 \end{bmatrix} \cdot \begin{bmatrix} S_{a1} \\ S_{b1} \\ S_{c1} \\ S_{a2} \\ S_{b2} \\ S_{c2} \end{bmatrix} \quad (1)$$

The stator phase voltages from (1) can in turn be expressed in the α-β and x-y subspaces using the power-invariant Clarke transformation matrix:

$$[C] = \frac{1}{\sqrt{3}} \cdot \begin{bmatrix} 1 & -1/2 & -1/2 & \sqrt{3}/2 & -\sqrt{3}/2 & 0 \\ 0 & \sqrt{3}/2 & -\sqrt{3}/2 & 1/2 & 1/2 & -1 \\ 1 & -1/2 & -1/2 & -\sqrt{3}/2 & \sqrt{3}/2 & 0 \\ 0 & -\sqrt{3}/2 & \sqrt{3}/2 & 1/2 & 1/2 & -1 \\ 1 & 1 & 1 & 0 & 0 & 0 \\ 0 & 0 & 0 & 1 & 1 & 1 \end{bmatrix} \quad (2)$$

$$[v_{\alpha s}\ v_{\beta s}\ v_{xs}\ v_{ys}\ v_{0+}\ \ v_{0-}]^T=[C][v_{a1}\ v_{b1}\ v_{c1}\ v_{a2}\ v_{b2}\ \ v_{c2}]^T$$

Applying the transformation matrix defined in (2), it is then possible to map the phase voltages into two orthogonal stationary subspaces, namely α-β and x-y, plus two zero-sequence components. The vector space decomposition (VSD) provides 64 (2^6) voltage vectors in these two orthogonal subspaces [24].

Finally, the α-β variables can be expressed in the d-q reference frame if the Park transformation matrix is applied. This transformation allows the independent regulation of the flux and the torque. The following Park transformation matrix is employed:

$$\begin{bmatrix} v_{ds} \\ v_{qs} \end{bmatrix} = \begin{bmatrix} \cos\theta_s & \sin\theta_s \\ -\sin\theta_s & \cos\theta_s \end{bmatrix} \cdot \begin{bmatrix} v_{\alpha s} \\ v_{\beta s} \end{bmatrix} \quad (3)$$

where θ_s is the angle of the reference frame and is calculated from the measured speed and the estimated slip [17].

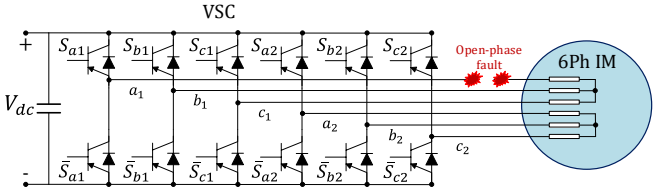

Fig. 1. Scheme of a six-phase IM drive, where an OPF occurrence is illustrated in phase a_1.

B. Six-phase induction machine with distributed windings

The six-phase IM can be represented by a set of differential equations. Although these equations are usually expressed in phase variables, the Clarke transformation matrix defined in (2) allows expressing the equations of the six-phase machine as a function of the VSD variables as follows [29]:

$$\begin{aligned} v_{\alpha s} &= \left(R_s + L_s\frac{d}{dt}\right) i_{\alpha s} + M\frac{di_{\alpha r}}{dt} \\ v_{\beta s} &= \left(R_s + L_s\frac{d}{dt}\right) i_{\beta s} + M\frac{di_{\beta r}}{dt} \\ v_{xs} &= \left(R_s + L_s\frac{d}{dt}\right) i_{xs} \\ v_{ys} &= \left(R_s + L_s\frac{d}{dt}\right) i_{ys} \\ 0 &= \left(R_r + L_r\frac{d}{dt}\right) i_{\alpha r} + M\frac{di_{\alpha s}}{dt} + \omega_r L_r i_{\beta r} + \omega_r M i_{\beta s} \\ 0 &= \left(R_r + L_r\frac{d}{dt}\right) i_{\beta r} + M\frac{di_{\beta s}}{dt} - \omega_r L_r i_{\alpha r} - \omega_r M i_{\alpha s} \\ T_e &= pM(i_{\beta r} i_{\alpha s} - i_{\alpha r} i_{\beta s}) \end{aligned} \tag{4}$$

where p is the number of pole pairs, $L_s = L_{ls} + 3{\cdot}L_m$, $L_r = L_{lr} + 3{\cdot}L_m$, $M = 3{\cdot}L_m$ and ω_r is the rotor electrical speed ($\omega_r = p{\cdot}\omega_m$). Subscripts s and r denote stator and rotor variables, respectively.

The mathematical modelling of the system shown in (4) provides an interesting advantage, since it is also valid when an open-phase fault occurs. The open-phase fault reduces the available degrees of freedom and makes the two orthogonal planes to be dependent. Consequently, the relationship between the VSD currents is modified with different constraints for each phase under fault. For example, assuming without lack of generality that the fault occurs in the phase a_1 (see Fig. 1), applying the Clarke transformation from (2) to phase currents and considering the fault restriction ($i_{a1} = 0$), the following post-fault restriction appears as a physical condition:

$$i_{xs} = -i_{\alpha s} \tag{5}$$

Nevertheless, in this fault situation there is still one extra freedom degree (the y-current). For this reason, in order to obtain a suitable performance in this post-fault situation, the most implemented solution is to define the reference value of the y-current according to a minimum loss or minimum derating criterion [20-22]. However, this paper focuses on the problems that appear if the control scheme is not modified. With this purpose, MPC and VV-MPC are implemented and evaluated.

III. Model-based Predictive Control

A. Model Predictive Control

The MPC technique is a popular alternative for the regulation of electrical machines that has exploded in recent years, particularly in the multiphase drives' field. This control method is based on the utilization of a discrete drive model (usually named as predictive model) to estimate the future values of the controlled stator currents. The predictive model must be iteratively evaluated every sampling time for each of the different available switching states. In this paper, a dual three-phase two-level VSC is employed and 49 independent switching states are available [24], being the computational cost an important constraint for the MPC implementation. This predictive model is generally expressed using the VSD variables, as shows in (6):

$$\begin{aligned} \frac{d}{dt}[X_{\alpha\beta xy}] &= [A]\cdot[X_{\alpha\beta xy}] + [B]\cdot[U_{\alpha\beta xy}] \\ [Y_{\alpha\beta xy}] &= [C]\cdot[X_{\alpha\beta xy}] \end{aligned} \tag{6}$$

where:

$$\begin{aligned} [U_{\alpha\beta xy}] &= [u_{\alpha s}\ u_{\beta s}\ u_{xs}\ u_{ys}\ 0\ 0]^T \\ [X_{\alpha\beta xy}] &= [i_{\alpha s}\ i_{\beta s}\ i_{xs}\ i_{ys}\ i_{\alpha r}\ i_{\beta r}]^T \\ [Y_{\alpha\beta xy}] &= [i_{\alpha s}\ i_{\beta s}\ i_{xs}\ i_{ys}\ 0\ 0]^T \end{aligned} \tag{7}$$

The matrices $[A]$, $[B]$ and [C], whose coefficients are dependent on the machine parameters, define the dynamics of a six-phase IM. A discretization technique derived from the Cayley-Hamilton equation is employed to obtain the predictive model [30].

The available switching states are evaluated in the predictive model, providing different stator currents ($\hat{\imath}_{\alpha\beta xy}$). The optimal switching state is obtained comparing the predicted and the reference stator currents using a predefined cost function (see Fig. 2a). The common version of the MPC technique uses an outer speed control loop to obtain the reference value of the q-current, whereas the d-current reference is usually defined as a constant value proportional to the rated flux. On the other hand, the reference values of the x-y currents are set to zero in machines with distributed windings, since these currents only provide additional copper losses. Applying the inverse of the Park transformation matrix defined in (3), the reference currents can be expressed in the α-β plane, and can be used in the cost function as follows:

$$J_1 = K_1\cdot e_{\alpha s}^2 + K_2\cdot {e_{\beta s}}^2 + K_3\cdot {e_{xs}}^2 + K_4\cdot {e_{ys}}^2 \tag{8}$$

where:

$$\begin{aligned} e_{\alpha s} &= (i_{\alpha s}^* - \hat{\imath}_{\alpha s}) \\ e_{\beta s} &= (i_{\beta s}^* - \hat{\imath}_{\beta s}) \\ e_{xs} &= (i_{xs}^* - \hat{\imath}_{xs}) \\ e_{ys} &= (i_{ys}^* - \hat{\imath}_{ys}) \end{aligned} \tag{9}$$

The K_i coefficients are the weighting factors for each component, which must be selected according to the control objective in pre-fault situation. The conventional MPC method presents an important disadvantage derived from the application of a single switching state during the whole sampling period. This fact provokes that the two orthogonal planes cannot be regulated in the same sample period regardless of how the weighting factors are selected in the cost function.

B. Model Predictive Control using Virtual Voltage Vectors

This section describes the MPC based on the utilization of VVs [24-25]. The nature of this MPC strategy is similar to the common MPC method, as it is shown in Fig. 2b. However, the use of VVs nullifies the average voltage values in the x-y plane. These VVs are obtained using medium-large and large voltage vectors with the same direction in the α-β plane [24-25]. Note however that these voltage vectors are in opposition in the x-y plane. Then, it is possible to obtain a set of twelve active VVs in the α-β plane with a null average value in the x-y plane [24]. For this purpose, the application time of these voltage vectors must be t_1=0.73 $\cdot\ T_m$ and t_2=0.27 $\cdot\ T_m$. For the sake of example, it can be observed in Fig. 3a that vectors 52 and 38 are aligned in the α-β plane (52 is large and 38 is medium-large) but opposed in the x-y plane (52 is small and is 38 is medium-large). By applying vector 52 during 73% of

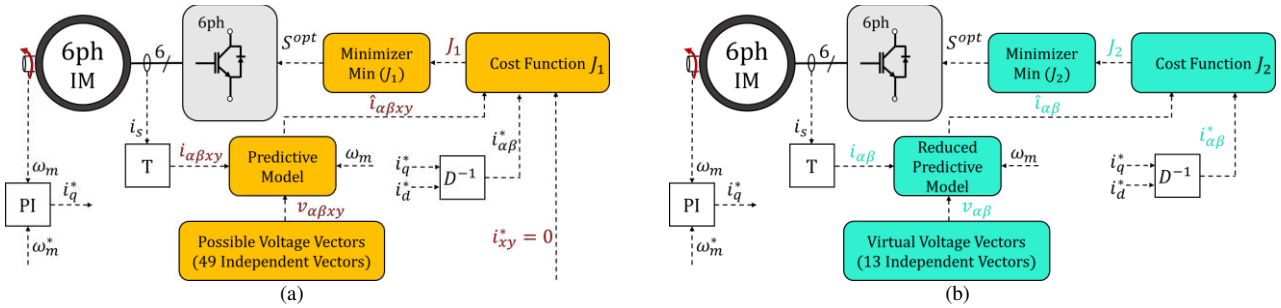

Fig. 2. Conventional MPC (a) and VV-MPC (b) control schemes for a six-phase IM.

the sampling period and vector 38 during 27% of the sampling period, the resulting average voltage in the x-y plane is null. This procedure can be extended to the different sectors to obtain a general expression for the VVs [24]:

$$VV_i = t_1 \cdot V_{large} + t_2 \cdot V_{medium-large} \quad (10)$$

With the application of these VVs, the control of the x-y currents is realized in open-loop, assuming that in a relatively well-balanced machine null x-y voltages will also lead to zero x-y currents. Machine asymmetries would eventually lead to non-null secondary currents and an associated lower efficiency, but this is not a foreseeable scenario since multiphase machines are built to be reasonably symmetrical (see experimental results in section V). Since there is no closed-loop control of the secondary components, they can be simply removed from the discrete model:

$$\frac{d}{dt}[X_{\alpha\beta}] = [\bar{A}] \cdot [X_{\alpha\beta}] + [\bar{B}] \cdot [U_{\alpha\beta}]$$
$$[Y_{\alpha\beta}] = [\bar{C}] \cdot [X_{\alpha\beta}] \quad (11)$$

where:

$$[U_{\alpha\beta}] = [u_{\alpha s}\ u_{\beta s}\ 0\ 0]^T$$
$$[X_{\alpha\beta}] = [i_{\alpha s}\ i_{\beta s}\ i_{\alpha r}\ i_{\beta r}]^T \quad (12)$$
$$[Y_{\alpha\beta}] = [i_{\alpha s}\ i_{\beta s}\ 0\ 0]^T$$

Following the same procedure, it is also possible to eliminate these components from the cost function:

$$J_2 = K_1 \cdot e_{\alpha s}^2 + K_2 \cdot {e_{\beta s}}^2 \quad (13)$$

To sum up, the VV-MPC presents the following advantages: application of null average vectors in the x-y plane, reduction of the computational cost due to definition of a new discrete model and cost-function, as well as the use of a lower number of iterations in every sampling time.

The MPC and VV-MPC techniques have been described in this section in pre-fault situation. Although, these two control methods have a similar nature, the control of the x-y components is realized using quite a different approach. Since this fact can be critical in the achievable post-fault performance, the next section examines why pre-fault MPC control strategies misbehave after the fault occurrence. It is worth noting that while [24-25] used the control scheme shown in Fig. 2b to demonstrate the benefits of VVs in healthy operation, the main focus of this work is to explore the additional advantages of VVs in post-fault situation. It follows that the subsequent analysis in faulty mode complements the one in [24-25] and jointly proves that VVs do not only improve current quality and efficiency in healthy state, but also provide natural means for a simplified fault-tolerant operation.

IV. Pre-Fault Control Scheme Problems in Post-Fault Situation

The reconfiguration of the control scheme is the most accepted regulation solution when a fault is detected in the system [4]. It is then firstly required to localize the fault (step 1) and then to modify the control scheme (step 2). Step 1 involves defining different fault indices and determining which type of open-phase fault exists [12]. For the sake of illustration, the number of fault scenarios in a n-phase machine with a single isolated neutral is equal to n for single phase faults and $(n-1)\cdot n/2$ for double phase faults. As a consequence, the number of scenarios dramatically increases as the number of phases in the machine gets higher (e.g. in a six-phase machine there are 6 single-fault scenarios and 15 double-fault scenarios whereas in a nine-phase machine there are 9 single-fault scenario and 36 double-fault scenarios). When using MPC, step 2 requires the modification of *i)* the Clarke transformation, *ii)* the cost function and *iii)* the current references for each of the aforementioned scenarios [18]. Although step 1 and 2 do not imply additional hardware, they clearly involve further complexity as the number of phases increases. Both the localization and control reconfiguration are mandatory because the pre-fault control strategies fail to provide a satisfactory performance after the fault. The objective of this section is to identify the problems in the controlled system when the open-phase fault appears.

From the point of view of the system operation, when the open-phase fault occurs the current cannot flow through the damaged phase. If the system does not detect the missing phase and the control action is not modified, the drive performance is affected to some extent due to the following reasons:

i) Search for incompatible goals: The OPF adds a new restriction to the system and, therefore, a degree of freedom is lost. As a consequence, the orthogonal α-β and x-y planes are no longer independent. However, if the control stage is not informed about the OPF occurrence, MPC still tries to minimize both $e_{\alpha\beta}$ (with $i_{\alpha\beta}^* \neq 0$) and e_{xy} (with $i_{xy}^* = 0$). In other words, the minimization of the terms in (8) is incompatible in nature. This conflict inevitably disturbs the regulation of α-β currents because both planes (α-β and x-y) are now linked (see Fig. 4). Therefore, the performance of the pre-fault MPC controller in post-fault situation is influenced by the relationship between α-β and x-y weighting factors.

It is worth highlighting that the aforementioned conflict can be overcome if the regulation of the x-y components is realized in open-loop. This is exactly what occurs with the use of VVs, since the x-y voltage production is zeroed. Since the cost function omits the x-y terms, as in (13), the conflict

disappears and MPC is not searching for incompatible goals anymore.

To sum up, while MPC requires the modification of the current references to avoid the conflict (this being the solution adopted in [16-18]), VV-MPC is a disturbance-free control strategy that inherently skips the conflict thanks to the open-loop regulation of the x-y currents.

ii) Available voltage vectors: The open-phase fault also changes the available voltage vectors. For this reason, all post-fault control schemes use different transformation matrices to obtain the new available voltage vectors. If the control scheme is not reconfigured after the fault, the selected voltage vector is erroneous and the control performance is degraded. Fig. 3 depicts the transition of normal and virtual voltage vectors from healthy (green circles) to faulty (red diamonds) operation when an open-phase fault occurs in phase a_1. Specifically, the error in the localization of the applied voltage vectors is shown using MPC technique (Fig. 3a) and VV-MPC method (Fig. 3b), where these localizations can slightly oscillate due to the back-EMF [17]. The displacement of the voltage vectors after the fault occurrence implies an error in the applied vector that contributes to the prediction's accuracy in the analyzed predictive controllers (see Fig. 2). It must be noted, however, that the use of MPC in normal operation already implies an error between the desired and the applied voltage vector due to the discrete nature of the converter and the absence of a modulation stage [31-33]. Consequently, the error in the selection of the voltage vector may have a low impact in the drive performance as long as the displaced vectors are still around the same sector in pre- and post-fault conditions.

In summary, this section has detailed the main problems that MPC controllers face if an open-phase fault occurs and the control action is not reconfigured.

V. Experimental Results

The objective of this section is to test the performance of VV-MPC in post-fault operation and to compare its performance with conventional MPC. The comparative experimental results will confirm the ability of VV-MPC to skip the control conflict and thus obtain a disturbance-free post-fault operation.

A. Test Bench

The employed test bench is depicted in Fig. 5. It includes an asymmetrical six-phase IM supplied from conventional two-level three-phase VSCs (Semikron SKS22F modules). The parameters of the custom-built six-phase IM have been obtained using ac-time domain and stand-still with inverter supply tests [34-35]. Table I shows the induction motor drive parameters and rated values.

A single dc power supplies the VSCs and the control actions are performed by a digital signal processor (TMS320F28335 from Texas Instruments, TI). The control unit is programmed using a JTAG and the TI proprietary software called Code Composer Studio. The current and speed measurements are obtained using four hall-effect sensors (LEM LAH 25-NP) and a digital encoder (GHM510296R/2500), respectively. The six-phase IM is loaded coupling its shaft to a dc machine that acts as a generator. The armature of the dc machine is connected to a variable passive R load that dissipates the power and the load torque is consequently speed-dependent.

B. Experimental Results

To start with, the performance of the conventional MPC must be evaluated in pre-fault situation to tune the applied weighting factors. These coefficients are selected on a trial and error basis to obtain suitable performance of the drive in normal operation, with good tracking of the reference variables and the lowest rms current. Different weighting factors were tested, and Fig. 6 summarizes the obtained results in three analysed cases (K_α=K_β=1 and K_x=K_y=[0.5; 0.1; 0.01]). It is visible that when weighting

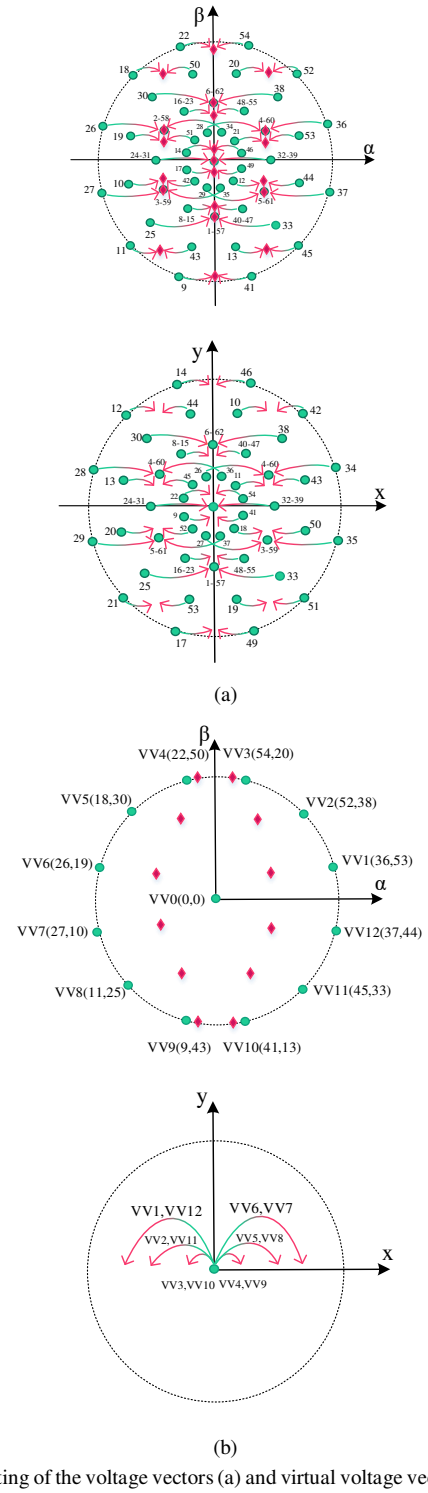

Fig. 3. Shifting of the voltage vectors (a) and virtual voltage vectors (b) when transiting from healthy (green circles) to faulty operation (red diamonds).

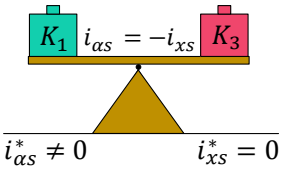

Fig. 4. Scheme of the control conflict after the OPF occurrence in phase a_1. K_1 and K_3 are the weighting factors of the α and x terms in the cost function, respectively. The objective of α-controller is $i^*_{\alpha s} \neq 0$, the objective of the x-controller is $i^*_{xs} = 0$ and the fault restriction is $i_{\alpha s} = -i_{xs}$.

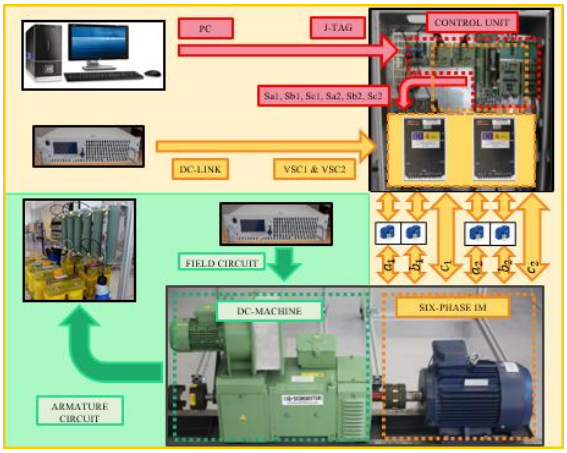

Fig. 5. Test bench

TABLE I

TEST-BENCH AND INDUCTION MOTOR DRIVE RATED PARAMETERS' VALUES

Power (kW)	0.8
Dc-link voltage (V)	200
Dead time (μs)	4
I_{peak} (A)	4.06
i_d (A)	0.8
i_q (A)	8
n_m (rpm)	1000
R_s (Ω)	14.2
R_r (Ω)	2
L_m (mH)	420
L_{ls} (mH)	21.5
L_{lr} (mH)	55

factors K_x and K_y are set at high values (0.5), the tracking of the d-q currents is affected (Fig. 6b, left plot) and when they are set to low values (0.01), then the ripple of the x-y currents becomes higher (Fig. 6c, right plot). Furthermore, the configuration that gives the lowest rms current value is K_α=K_β=1 and K_x=K_y=0.1, as it is shown in Table II. For these reasons, this weighting factor relationship is employed with the conventional MPC in what follows.

A second test is done to compare the transition from pre- to post-fault situation using the conventional and VV-based MPC techniques. An open-phase fault is forced in phase a_1 for the sake of simplicity (see Fig. 7c). Fig. 7 summarizes the obtained results, where three control methods are analysed:

- The proposed VV-MPC technique that uses virtual vectors (see left column in Fig. 7).
- A conventional MPC method with the weighting factors selected in test 1 (i.e. K_α=K_β=1 and K_x=K_y=0.1) or MPC-1 (see middle column in Fig. 7).
- The conventional MPC method with null x-y weighting factors (i.e. K_α=K_β=1 and K_x=K_y=0) or MPC-0 (see right column in Fig. 7).

While the three control methods provide a suitable speed and d-q current regulation in normal operation, as it is shown in Figs. 7a and 7b, MPC-0 offers an excessive phase current distortion because x-y currents are not controlled (see Fig. 7e and 7c, right plots). Specifically, the THD of phase currents with MPC-0 is more than 3.5 times higher than using VV-MPC (31.38% versus 8.62% for phase currents shown in the left and right plots of Fig. 7c). Comparing MPC-1 and VV-MPC, it is noticeable that the lowest current ripple both in x-y (Fig. 7e) and phase currents (Fig. 7c) corresponds to the VV-MPC technique, which confirms the benefits of using VVs detailed in [24]. It can then be concluded that the elimination of the x-y weighting factor (MPC-0) is not viable due to large copper losses and low efficiency, whereas MPC-1 is viable but at the cost of a significantly poorer closed-loop performance than using VV-MPC. It is worth highlighting that the x-current can no longer be regulated near zero in post-fault situation because the OPF restriction from (5) forces i_x to be -i_α. In other words, the loss of one degree of freedom when phase a_1 is open implies that the x-current cannot be independently regulated as in pre-fault condition. On the contrary, the y-current can still be regulated to values near zero following a minimum copper loss (MCL) criterion [14, 19,23]. The unavoidable appearance of the x-current after the OPF occurrence increases the stator copper losses [14], which in turn implies a lower efficiency. As a consequence, the drives need to be derated and the maximum α-β currents are limited to 55.5% of the pre-fault values for single OPF under MCL operation with two isolated neutrals. Further details about the post-fault copper losses and drive derating for other configurations and fault scenarios are available in [19].

Focusing in the transition from pre- to post-fault situations, at t=10 s an open-phase fault is forced in phase a_1 and therefore the system losses one degree of freedom. The two orthogonal subspaces are no longer independent due to the fault constraint because i_x=−i_α (see Figs. 7d and 7e). It is highly noticeable the obtained disturbance in d-q currents and the drop in the transient speed using MPC-1 (see Figs. 7a and 7b) caused by the conflict between x-y terms of the cost function (e_{xs} and e_{ys}) and the new post-fault restriction (see section IV for further details). Interestingly enough, MPC-1 is the unique control method affected during the transition because x-y currents are controlled in a closed-loop manner. This conflict also generates an offset and huge ripple in d-q currents in post-fault operation, as it is shown in the middle column of Fig. 7b. Since the flux and torque generation in distributed-winding multiphase machines is purely dependent on the d-q currents, the torque ripple with MPC-1 becomes more than three times higher compared to VV-MPC (see Fig. 7f). On the contrary, these two phenomena do not appear when VV-MPC or MPC-0 are used (see left and right columns of Figs. 7a and 7b, where no speed drop and good regulation of d-q currents are achieved in post-fault situation). This improvement in the performance after the fault occurrence is achieved because x-y currents are not closed-loop controlled. Even though MPC-0 achieves a natural fault tolerance, this property comes at the expense of a poor current quality in normal operation of the electric drive (see Fig. 7c).

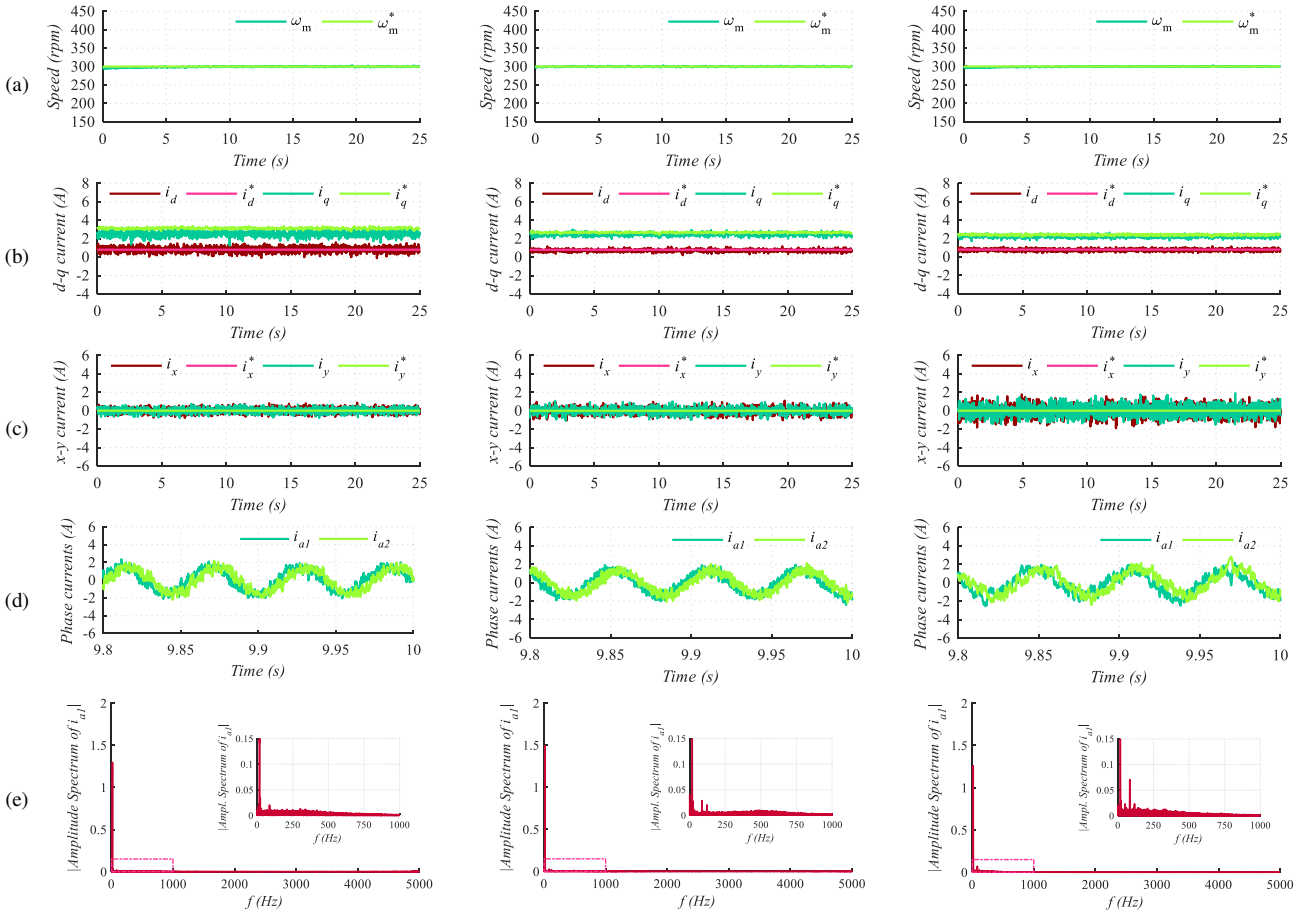

Fig. 6. Test 1. Performance of MPC with K_α=K_β=1 and K_x=K_y=0.5 (left column), MPC with K_α=K_β=1 and K_x=K_y=0.1 (middle column) and MPC with K_α=K_β=1 and K_x=K_y=0.01 (right column) in healthy situation. From top to bottom: a) motor speed, b) d-q currents, c) x-y currents, d) phase currents and e) frequency spectrum of the phase-current a_1.

TABLE II
TEST 1: RMS CURRENTS WITH CONVENTIONAL MPC METHOD

Weighting factors	Phase currents rms value (A)
K_α=K_β=1 and K_x=K_y=0.50	1.8580
K_α=K_β=1 and K_x=K_y=0.10	1.1192
K_α=K_β=1 and K_x=K_y=0.01	1.1324

Since MPC-0 and MPC-1 do not provide a satisfactory performance in pre- and post-fault situations, respectively, it can then be concluded that the VV-MPC technique is the unique method that provides a suitable performance in normal, faulty and transitory operations. Table III qualitatively compares the performance of the drive using VV-MPC, MPC-1 and MPC-0 during normal, open-phase fault and transitory states (green, orange and red colours depict high, medium and low performance characteristics, respectively).

It is worth highlighting that both MPC-0 and VV-MPC satisfactorily regulate d-q currents in spite of using the erroneous pre-fault voltage vectors shown in Fig. 3, confirming that the main problem after the fault occurrence is not the shifting of the voltage vectors, but the conflict caused by the incompatible goals in d-q and x-y planes. Finally, it must be noted that the post-fault performance follows the minimum copper loss criterion (ML) mode of operation described in literature [4], and there is no possibility to select other criteria at will because there is no control reconfiguration. In any case, the ML mode promotes efficiency and minimizes the drive derating when copper losses are kept constant after the fault occurrence, so the post-fault performance can be regarded as satisfactory.

The dynamic response using the proposed VV-MPC technique is analysed next in post-fault operation (again an open-phase fault in phase a_1 is considered). A speed reversal test is performed changing the speed reference from 300 rpm to -300 rpm (Fig. 8a), producing a variation in the q-current reference while the d-current remains constant during the test (see Fig. 8b). However, regardless of the behaviour of these currents, their regulation is satisfactorily done. Fig. 8c shows the waveform of α-β currents during the test and, as expected, the variation of the α-current produces a change in the x-current due to the constraint of the open-phase fault (see Fig. 8d).

The performance of the proposed VV-MPC method is finally evaluated when two open-phase faults are forced. Two simultaneous open-phase faults are provoked in phases a_1 and c_2 at t=10s, as shown in Fig. 9c. Although two open-phase faults occur, the tracking of the reference speed ($800\,rpm$) is adequate (see Fig. 9a). As expected, x-y currents are null during the pre-fault operation. However, x-y currents deviate from their previous null values when the faults are forced due to the new post-fault restrictions (see Fig. 9d). Fig. 9b shows a small variation in d-q currents when the faults occur. This variation is due to the mentioned displacement in the VVs' localization during the post-fault operation. Regardless this error, it is highly noticeable that the VV-MPC method offers a satisfactory performance even in this severe post-fault scenario.

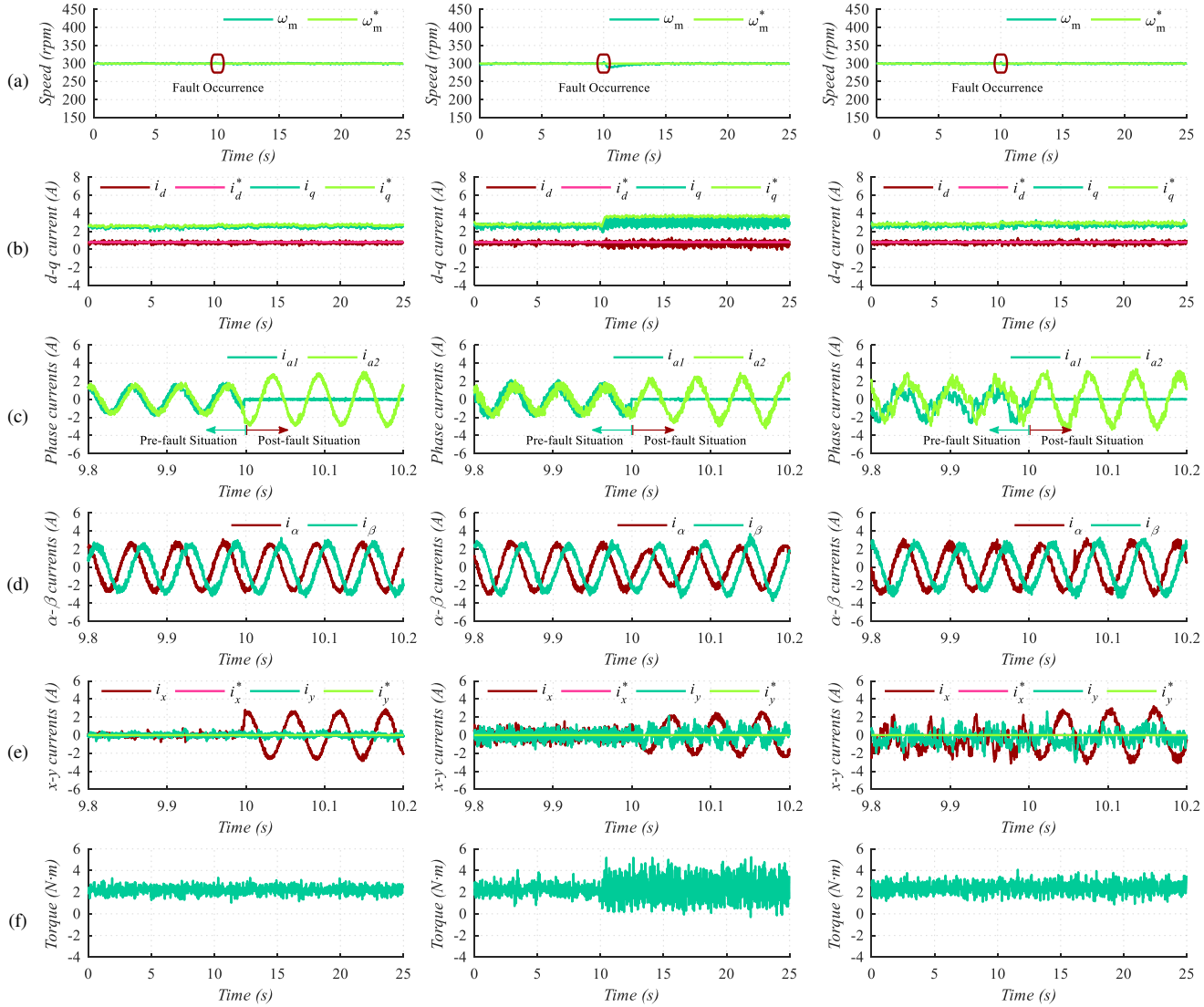

Fig. 7. Test 2. Transition from pre- to post-fault situation when an open-phase fault occurs using VV-MPC (left column), MPC-1 with K_α=K_β=1 and K_x=K_y=0.1 (middle column) and MPC-0 with K_α=K_β=1 and K_x=K_y=0 (right column). From top to bottom: a) motor speed, b) d-q currents, c) phase currents d) α-β currents, e) x-y currents and f) electromagnetic torque,

TABLE III

TEST 2: A QUALITATIVE COMPARISON BETWEEN VV-MPC, MPC-1 AND MPC-0 TECHNIQUES IN NORMAL, FAULTY AND TRANSITORY (FROM PRE- TO POST-FAULT SITUATION) OPERATION

Control Methods	Pre-fault situation	Transition situation	Post-fault situation
VV-MPC	⇑⇑	⇑⇑	⇑⇑
MPC-1 (with K_α=K_β=1 and K_x=K_y=0.1)	⇑	⇓	⇓⇓
MPC-0 (with K_α=K_β=1 and K_x=K_y=0)	⇓⇓	⇑⇑	⇓

All in all, the experimental results confirm the ability of VV-MPC to operate in post-fault situation even with no control reconfiguration. This natural fault-tolerant capability has significant benefits for industrial applications:

- Simplicity: the fault localization is not required to obtain a disturbance-free post-fault operation. Hence, there is no need to identify all possible fault scenarios and store off-line a control reconfiguration for each specific case.
- Computational cost: it is well-known that real-time implementation of MPC in multiphase systems becomes challenging due to the high computational cost involved. While the standard fault-tolerant approach places an additional burden, the lack of reconfiguration together with the reduced-order model eases the real-time implementation of VV-MPC.
- Immunity to fault detection errors and delays: it is reported in literature that fault detection delays severely affect the transition from pre- to post-fault situations with high torque/speed ripple [18]. Furthermore, fault detection methods are not infallible and any error in the fault localization might damage the multiphase drive. Fortunately, the natural fault-tolerance that can be achieved with VV-MPC safeguards the drive integrity because the disturbance-free post-fault performance is guaranteed.

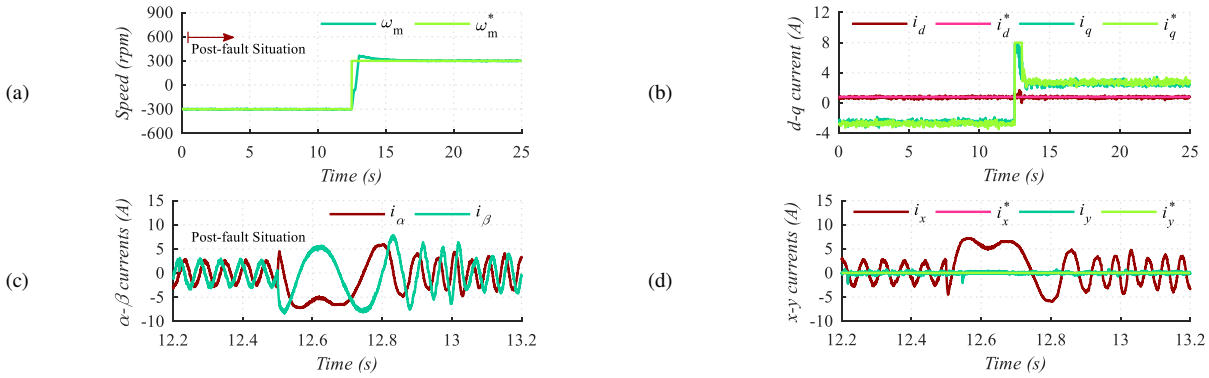

Fig. 8. Test 3. Speed reversal test using VV-MPC. From top to bottom and left to right: a) motor speed, b) d-q currents, c) phase currents and d) x-y currents.

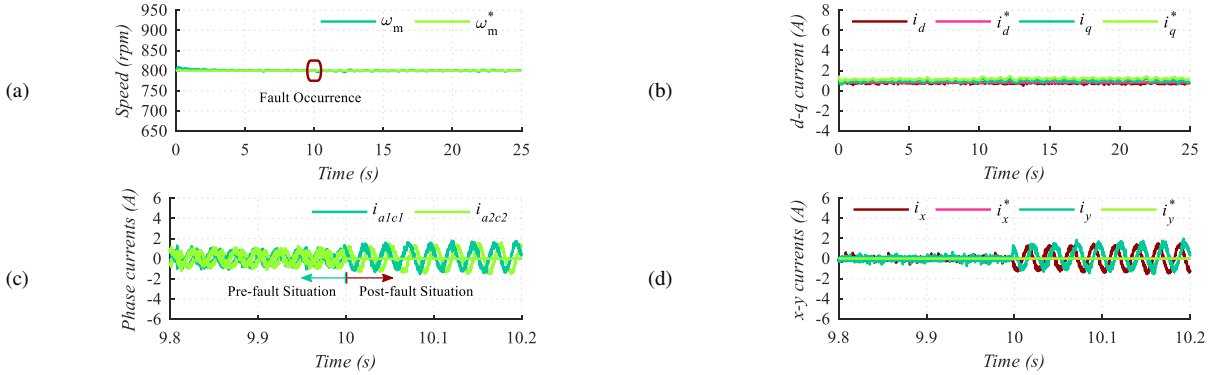

Fig. 9. Test 4. Transition from pre to post-fault situation when two open-phase faults occur using the VV-MPC technique. From left to right and from top to bottom a) motor speed, b) d-q currents, c) phase currents and d) x-y currents.

VI. Conclusions

The use of modern drives in industry applications requires not only the definition of high-performance controllers but also the automatic management of fault appearances, being the latter a very important issue in recent research works where open-phase faults are usually considered. This work focuses on the fault tolerance analysis of high-performance drives based on multiphase machines, where two main reasons can cause a low performance of the system after the OPF occurrence: the shifting of the voltage vectors and the conflict between α-β and x-y controllers. While the former has a low impact on the control performance if voltage vectors are still in the same sector, the latter can seriously disturb the current regulation because α-β and x-y terms in the cost function have incompatible objectives. A simple solution to avoid current regulation disturbances in MPC-based schemes is to cancel the weighting factors of x-y currents. Unfortunately, releasing the x-y current control results in unacceptable current ripple and high copper losses. A more elaborated manner to obtain ripple-free d-q current control is to use virtual voltage vectors instead of applying a single switching state during the whole sampling period. With this procedure the x-y currents are regulated to be near zero in open-loop mode, thus avoiding the conflict caused by the fault restriction.

It is revealed in this work that the MPC-based controller using virtual voltage vectors (VV-MPC) provides the drive with a natural fault-tolerant capability (i.e. a ripple-free post-fault performance without any extra control reconfiguration). This in turn provides a smoother transient from pre- to post-fault operation and makes the control immune to fault detection errors or delays.

VII. Acknowledgment

The authors gratefully acknowledge the contribution of Prof. E. Levi for the suggestion of the term natural fault tolerance that is used in this work.

References

[1] E. Levi, “Multiphase Machines for Variable-Speed Applications”, *IEEE Trans. on Ind. Electron.*, vol. 55, no. 5, pp. 1893-1909, 2008.

[2] E. Levi, R. Bojoi, F. Profumo, H.A. Toliyat and S. Williamson, “Multiphase induction motor drives - a technology status review,” *IET Electric Power Appli.*, vol. 1, no. 4, pp. 489-516

[3] Z. Liu, Y. Li and Z Zheng, “A review of drive techniques for multiphase machines,” *CES Trans. on Electrical Machines and Systems*, vol. 2, no. 2, pp. 243-251, 2018.

[4] E. Levi, “Advances in converter control and innovative exploitation of additional degrees of freedom for multiphase machines,” *IEEE Trans. Ind. Electron.*, vol 63, no. 1, pp. 433-448, 2016.

[5] “Gamesa 5.0 MW” Gamesa Technological Corporation S.A., 2016. Online available: http://www.gamesacorp.com/recursos/doc/

[6] I. Gonzalez-Prieto, M.J. Duran, H.S. Che, E. Levi and F. Barrero “Fault-tolerant operation of six-phase energy conversion systems with parallel machine-side converters,” *IEEE Trans. Power Electron.*, vol. 31, no. 4, pp. 3068-3079, 2016.

[7]] M.J. Duran, E. Levi and F. Barrero, Multiphase Electric Drives: Introduction, Wiley Encyclopedia of Electrical and Electronics Engineering, pp. 1–26, 2017.

[8] J. O. Estima and A. J. M. Cardoso, “A new algorithm for real-time multiple open-circuit fault diagnosis in voltage-fed PWM motor drives by the reference current errors,” *IEEE Trans. Ind. Electron.*, vol. 60, no. 8, pp. 3496–3505, 2013.

[9] N. M. A. Freire, J. O. Estima, and A. J. M. Cardoso, “Open-circuit fault diagnosis in PMSG drives for wind turbine applications,” *IEEE Trans. Ind. Electron*., vol. 60, no. 9, pp. 3957–3967, 2013.

[10] L. Zarri, M. Mengoni, Y. Gritli, A. Tani, F. Filippetti, G. Serra and D. Casadei, “Detection and localization of stator resistance dissymmetry based on multiple reference frame controllers in multiphase induction motor drives,” *IEEE Trans. Ind. Electron.*, vol. 60, no. 8, pp. 3506-3518, 2013.

[11] M. Trabelsi, N.K. Nguyen and E. Semail,"Real-time switches fault diagnosis based on typical operating characteristics of five-phase permanent-magnetic synchronous machines," *IEEE Trans. Ind. Electron.*, vol. 63, no. 8, pp. 4683-4694, 2016.

[12] I. Gonzalez-Prieto, M.J. Duran, N. Rios, F. Barrero and C. Martin, "Open-switch fault detection in five-phase induction motor drives using model predictive control" *IEEE Trans. Power Electron.,* vol. 65, no. 4, pp. 3045-3055, 2017.

[13] H.S. Che, E. Levi, M. Jones, M.J. Duran, W.P. Hew, and N.A. Rahim, "Operation of a six-phase induction machine using series-connected machine-side converters," *IEEE Trans. Ind. Electron.*, vol. 61, no. 1, pp. 164-176, 2014.

[14] H.S. Che, M.J. Duran, E. Levi, M. Jones, W.P. Hew and N.A. Rahim, "Post-fault operation of an asymmetrical six-phase induction machine with single and two isolated neutral points," *IEEE Trans. on Power Electron.*, vol. 29, no. 10, pp. 5406-5416, 2014.

[15] M. Bermudez, I. Gonzalez-Prieto, F. Barrero, H. Guzman, M.J.Duran and X. Kestelyn, "Open-phase fault-tolerant direct torque control technique for five-phase induction motor drives," *IEEE Trans. Ind. Electron.,* vol 64, no. 2, pp. 902-911, 2017.

[16] M. Bermudez, I. Gonzalez-Prieto, F. Barrero, H. Guzman, X. Kestelyn and M.J.Duran, "An experimental assessment of open-phase fault-tolerant virtual-vector-based direct torque control in five-phase induction motor drives," *IEEE Trans. on Power Electron.*, vol 33, no. 3, pp. 2774-2784, 2017.

[17] H. Guzmán, F. Barrero and M.J. Duran, "IGBT-gating failure effect on a fault-tolerant predictive current controlled 5-phase induction motor drive," *IEEE Trans. on Ind. Electron.*, vol 62, no. 1, pp. 15-20, 2015.

[18] H. Guzmán, M.J. Durán, F. Barrero, L. Zarri, B. Bogado, I. González and M.R. Arahal, "Comparative study of predictive and resonant controllers in fault-tolerant five-phase induction motor drives," *IEEE Trans. on Ind. Electron.*, vol 63, no. 1, pp. 606-617, 2016.

[19] W. N. W. A. Munim, M. J. Duran, H. S. Che, M. Bermudez, I. G.-Prieto and N. A. Rahim, "A unified analysis of the fault tolerance capability in six-phase induction motor drives," *IEEE Trans. Power Electron*., vol. 32, no. 10, pp. 7824-7836, 2017.

[20] F. Baneira, J. Doval-Gandoy, A. G. Yepes, Ó. López and D. Pérez-Estévez, "Control strategy for multiphase drives with minimum losses in the full torque operation range under single open-phase fault," *IEEE Trans. Power Electron.,* vol. 32, no. 8, pp. 6275-6285, 2017.

[21] F. Baneira, J. Doval-Gandoy, A. G. Yepes, Ó. López and D. Pérez-Estévez, "Comparison of post-fault strategies for current reference generation for dual three-phase machines in terms of converter losses," *IEEE Trans. Power Electron.,* vol. 32, no. 11, pp. 8243-8246, 2017.

[22] A. Tani, M. Mengoni, L. Zarri, G. Serra and D. Casadei "Control of multiphase induction motors with an odd number of phases under open-circuit phase faults," *IEEE Trans. Power Electron.,* vol. 27, no. 2, pp. 565-577, 2012.

[23] A. G. Yepes, J. Doval-Gandoy, F. Baneira and H. A. Toliyat, "Control strategy for dual three-phase machines with two open phases providing minimum loss in the full torque operation range", *IEEE Trans. on Power Electron.*, vol. 33, no. 12, pp. 10044-10050, 2018.

[24] I. Gonzalez-Prieto, M. J. Duran, J. J. Aciego, C. Martin and F. Barrero, "Model predictive control of six-phase induction motor drives using virtual voltage vectors,"*IEEE Trans. on Ind. Electron.*, vol 65, no. 1, pp. 27-37, 2018.

[25] C. Xue, W. Song and X. Feng, "Finite control-set model predictive current control of five-phase permanent-magnet synchronous machine based on virtual voltage vectors," *IET Electric Power Appl.*, vol. 11, no. 5, pp. 836-846, 5 2017.

[26] J. K. Pandit, M. V. Aware, R. Nemade and Y. Tatte, "Simplified implementation of synthetic vectors for DTC of asymmetric six-phase induction motor drives," *IEEE Trans. on Ind. Appl.*, vol. 54, no. 3, pp. 2306-2318, 2018.

[27] Y. Ren and Z. Q. Zhu, "Enhancement of steady-state performance in direct-torque-controlled dual three-phase permanent-magnet synchronous machine drives with modified switching table," *IEEE Trans. on Ind. Electron.*, vol. 62, no. 6, pp. 3338-3350, 2015.

[28] Y. Ren and Z. Q. Zhu, "Reduction of both harmonic current and torque ripple for dual three-phase permanent-magnet synchronous machine using modified switching-table-based direct torque control," *IEEE Trans. on Ind. Electron.*, vol. 62, no. 11, pp. 6671-6683, 2015.

[29] Y. Zhao and T. A. Lipo, "Space vector PWM control of dual three-phase induction machine using vector space decomposition," *IEEE Trans. Ind. Appl*., vol. 31, no. 5, pp. 1100–1109, 1995.

[30] C. Martín, M. R. Arahal, F. Barrero, and M. J. Duran, "Five-phase induction motor rotor current observer for finite control set model predictive control of stator current," *IEEE Trans. Ind. Electron.*, vol. 63, no. 7, pp. 4527–4538, 2016

[31] M. Lopez, J. Rodriguez, C. Silva, and M. Rivera, "Predictive Torque control of a multidrive system fed by a dual indirect matrix converter," *IEEE Trans. Ind. Electron*., vol. 62, no. 5, pp. 2731–2741, 2015.

[32] S. Kouro, M. A. Perez, J. Rodriguez, A. M. Llor, and H. A. Young,"Model predictive control: MPC's role in the evolution of power electronics," *IEEE Ind. Electron. Mag*., vol. 9, no. 4, pp. 8–21, 2015.

[33] C. S. Lim, E. Levi, M. Jones, N. A. Rahim, and W. P. Hew, "FCS-MPC based current control of a five-phase induction motor and its comparison with PI-PWM control," *IEEE Trans. Ind. Electron*., vol. 61, no. 1, pp. 149–163, Jan. 2014.

[34] A. Yepes, J.A. Riveros, J. Doval-Gandoy, F. Barrero, O. Lopez, B. Bogado, M. Jones and E. Levi, "Parameter identification of multiphase induction machines with distributed windings-part 1: sinusoidal excitation methods," *IEEE Trans. on Energy Conv.*, vol. 27, no. 4, pp. 1056-1066, 2012.

[35] J.A. Riveros, A. Yepes, F. Barrero, J. Doval-Gandoy, B. Bogado, O. Lopez, M. Jones and E. Levi, "Parameter identification of multiphase induction machines with distributed windings-part 2: time-domain techniques," *IEEE Trans. on Energy Conv*., vol. 27, no. 4, pp. 1067-1077, 2012.

Ignacio González Prieto was born in Malaga, Spain, in 1987. He received the Industrial Engineer and M.Sc. degrees in fluid mechanics from the University of Malaga, Malaga, Spain, in 2012 and 2013, respectively, and the Ph.D. degree in electronic engineering from the University of Seville, Sevilla, Spain, in 2016. His research interests include multiphase machines, wind energy systems, and electrical vehicles

Mario J. Duran was born in Bilbao, Spain, in 1975. He received the M.Sc. and Ph.D. degrees in electrical engineering from the University of Malaga, Malaga, in 1999 and 2003, respectively. He is currently a Full Professor in the Department of Electrical Engineering, University of Malaga. His research interests include modeling and ´ control of multiphase drives and renewable energies conversion systems.

Mario Bermudez was born in Málaga, Spain, in 1987. He received the B.Eng. degree in industrial engineering from the University of Málaga, Málaga, Spain, in 2014, and the Ph.D. degree in electrical/electronic engineering jointly from Arts et Métiers ParisTech, Lille, France, and from the University of Seville, Seville, Spain, in 2018. He is currently a Substitute Professor in the Department of Electrical Engineering, University of Huelva, Huelva, Spain. His research interests include modeling and control of multiphase drives, digital signal processor-based systems, and electrical vehicles.

Federico Barrero (M 04; SM 05) received the MSc and PhD degrees in Electrical and Electronic Engineering from the University of Seville, Spain, in 1992 and 1998, respectively. In 1992, he joined the Electronic Engineering Department at the University of Seville, where he is currently a Full Professor. He received the Best Paper Awards from the IEEE Trans. on Ind. Electron. for 2009 and from the IET Electric Power Applications for 2010-2011.

Cristina Martín was born in Seville, Spain, in 1989. She received the Industrial Engineer degree from the University of Málaga, Spain, in 2014. In 2015, she joined the Electronic Engineering Department of the University of Seville, where she is currently working toward the Ph.D. degree. Her current research interests include modeling and control of multiphase drives, microprocessor and DSP device systems, and electrical vehicles.